Hindawi Publishing Corporation
Mathematical Problems in Engineering
Volume 2013, Article ID 383947, 11 pages
http://dx.doi.org/10.1155/2013/383947

Research Article

Equivalent Representation Form of Oscillators with Elastic and Damping Nonlinear Terms

Alex Elías-Zúñiga,[1] Daniel Olvera,[1] Inés Ferrer Real,[2] and Oscar Martínez-Romero[1]

[1] *Centro de Innovación en Diseño y Tecnología, Tecnológico de Monterrey, Campus Monterrey, E. Garza Sada 2501 Sur, 64849 Monterrey, NL, Mexico*
[2] *Department of Mechanical Engineering and Industrial Construction, University of Girona, Maria Aurelia Capmany 61, 17071 Girona, Spain*

Correspondence should be addressed to Alex Elías-Zúñiga; aelias@itesm.mx

Received 22 July 2013; Revised 17 September 2013; Accepted 17 September 2013

Academic Editor: Miguel A. F. Sanjuán

In this work we consider the nonlinear equivalent representation form of oscillators that exhibit nonlinearities in both the elastic and the damping terms. The nonlinear damping effects are considered to be described by fractional power velocity terms which provide better predictions of the dissipative effects observed in some physical systems. It is shown that their effects on the system dynamics response are equivalent to a shift in the coefficient of the linear damping term of a Duffing oscillator. Then, its numerical integration predictions, based on its equivalent representation form given by the well-known forced, damped Duffing equation, are compared to the numerical integration values of its original equations of motion. The applicability of the proposed procedure is evaluated by studying the dynamics response of four nonlinear oscillators that arise in some engineering applications such as nanoresonators, microresonators, human wrist movements, structural engineering design, and chain dynamics of polymeric materials at high extensibility, among others.

1. Introduction

The aim of this paper focuses on using a nonlinear approach to transform the forced nonlinear equation:

$$\ddot{x} + f(x) + f_1\left(\nu\dot{x}, \kappa\dot{x}^p\right) = Q_0 \cos\left(\omega_f t\right), \quad x(0) = x_0, \ \dot{x}(0) = 0, \tag{1}$$

with nonlinear damping terms into an equivalent forced, linearly damped Duffing's equation. Here we assume that $f(x)$ is the system restoring force which could have rational or irrational conservative force terms, $f_1(\nu\dot{x}, \kappa\dot{x}^p)$ represents the system nonlinear dissipative effects, ν and κ are damping constants, p is the exponent of the velocity, Q_0 is the driving force magnitude, ω_f is the system driving frequency, t is the current time, and x_0 is the initial amplitude. The main motivation in studying the equivalent representation form of (1) with nonlinear damping terms for which $p > 0$ comes from the fact that the addition of nonlinear damping to the system could remove undesirable effects over the nonresonant regions that can help to improve the overall performance of Duffing-type vibration isolators [1, 2]. Furthermore, during the study of the dynamics response of resonators made from carbon nanotubes and graphene, Lifshitz and Cross [3] and Eichler et al. [4] concluded that damping is strongly dependent on the amplitude of motion and that its effects are better described by nonlinear damping forces. They also concluded that the nonlinearities could be associated with a dissipation channel exterior to the resonator, such as the manner in which the resonator is clamped by its boundaries to the surrounding material, friction effects associated with the sliding between the nanotube/graphene and the metal electrode, and the phonon-phonon interactions, among others. To quantify the nonlinear dissipative effects observed during

the performance of micromechanical oscillators, Zaitzev and coworkers designed a doubly clamped beam oscillator and performed several experimental studies to understand the phenomenon of nonlinear damping. They found that nonlinear damping plays an important role in the dynamics response of the micromechanical beam oscillator [5].

On the other hand, it is known that structural engineering design utilizes nonlinear damper devices to reduce the forces exerted in the dampers that could exceed the device force capacity during the structure dynamics response to earthquakes. In this case, the exponent of the velocity is selected on the interval of $0.3 < p < 1.95$ [6]. Martínez-Rodrigo and Romero [7] found that when the nonlinear dampers velocity exponent p is slightly less that 1, the forces in the dampers can be reduced more than 35% during the retrofitting of a multistory that leads to a similar structural performance when compared to the usage of linear dampers. Similar results were reported in [8] in which the utilization of nonlinear viscous dampers reduces the displacement response of existing girder bridges and arch bridge structures.

Since nonlinear dampers with fractional powers in the velocity terms are commonly used to model the rhythmic movement of the wrist, the inclusion of a nonlinear damping term for which $p = 1/5$ is considered in (1). This dynamics model is known as the one-fifth power law model [9]. Of course, there are other models that consider different values of p to characterize the damping and the elastic nonlinearities observed in different experimental measurements [10–12]. In an attempt to cover the gap between viscous, dry friction, and drag forces in turbulent fluids, Litak and coworkers considered a nonlinear damping term with a fractional exponent to model the behavior of double well oscillators. They identified the critical values of Q_0 that induced chaotic vibrations in the double well system with a nonlinear damping term [13]. Later, Borowiec and coworkers applied the Melnikov criterion to examine the global homoclinic bifurcation and the transition to chaos in a forced Duffing oscillator with nonlinear fractional damping term. They found, by using perturbation methods, the critical forcing amplitude above from which the system can behave chaotically [14].

It is clear that the inclusion of nonlinear damping terms in (1) allows a better prediction of the system dynamics response behavior [15–23]. Therefore, the aim of this paper focuses on modifying the nonlinear transformation approach introduced in [24] to find the equivalent representation form of (1) in which nonlinear damping with velocity terms to the power p is included.

2. A Nonlinear Transformation Procedure

To transform (1) into a driving, linearly damped differential equation of the Duffing type, we will follow the procedure introduced in [24] and consider first the transformation of the conservative force terms $f(x)$, which do not have a cubic-like representation form, by using the classical Chebyshev polynomials of the first kind [25–29], since this provides a uniform approximation and requires a smaller number of expansion terms in comparison, for instance, to Taylor series to obtain good accuracy [30]:

$$f(x) = \sum_{n=0}^{N} b_{2n+1}(x)\, T_{2n+1}(x), \tag{2}$$

where

$$b_{2n+1} = \frac{2}{\pi}\int_{-1}^{+1} \frac{1}{\sqrt{1-x^2}} f(x)\, T_{2n+1}(x)\, dx, \tag{3}$$

and T_{2n-1} are the Chebyshev polynomials of the first kind defined as

$$T_{2n+1}(x) = \cos\left[(2n+1)\cos^{-1}(x)\right], \quad x \in [-1,1],\ n = 0,1,2,\ldots. \tag{4}$$

The first three terms are given by

$$T_1(x) = x, \qquad T_3(x) = 4x^3 - 3x, \qquad T_5(x) = 16x^5 - 20x^3 + 5x. \tag{5}$$

Thus, the equivalent restoring force $f(x)$ can be written as

$$f(x) \equiv b_1(q)\, T_1(y) + b_3(q)\, T_3(y) \approx \alpha(A)\, x + \beta(A)\, x^3 + \gamma(A)\, x^5. \tag{6}$$

Substituting (2) into (3), by using (5), provides the following equivalent representation form of $f(x)$:

$$f(x) \approx \alpha(x)\, x + \beta(x)\, x^3 + \gamma(x)\, x^5. \tag{7}$$

Then, (1) can be equivalently written as

$$\frac{d^2x}{dt^2} + \alpha(x)\, x + \beta(x)\, x^3 + \gamma(x)\, x^5 + f_1\left(\nu\dot{x}, \kappa\dot{x}^p\right) - Q_0\cos\left(\omega_f t\right) \approx 0. \tag{8}$$

Since nonlinear damping terms are involved in the dissipative force expression $f_1(\nu\dot{x}, \kappa\dot{x}^p)$, we modify our cubication nonlinear transformation approach introduced in [24] by adding a constant term $c(x)$ to the resulting Duffing equation. This term will take into account the asymmetric dynamics behavior described by (1) due to the presence of the nonlinear dissipative effects. For instance, let us consider the forced Duffing equation with nonlinear damping terms:

$$\ddot{x} + \nu\dot{x} + \kappa_0\dot{x}|\dot{x}|^{p-1} + \alpha x + \beta x^3 = Q_0\cos\left(\omega_f t\right), \quad \text{with } x(0) = x_0,\ \dot{x}(0) = 0, \tag{9}$$

where y denotes the displacement of the system, ν and κ_0 are damping coefficients, α, β, and Q_0 are system constant parameters, and ω_f represents the driving frequency. Figure 1 shows the phase portrait of (1) by considering the values of $p = 1$ and 2.5. Notice that when $p \neq 1$, the corresponding phase portrait exhibits asymmetric dynamic behavior about

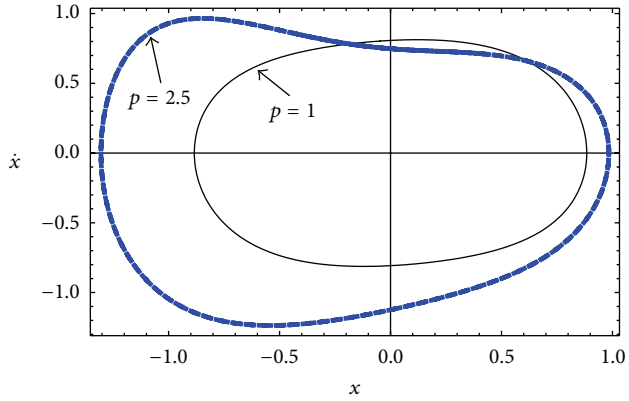

FIGURE 1: Steady-state phase portraits of $\ddot{x} + \nu\dot{x} + \kappa_0\dot{x}|\dot{x}|^{p-1} + \alpha x + \beta x^3 = Q_0\cos(\omega_f t)$ when $\alpha = 1$, $\beta = 1$, $\nu = 0.1$, $\kappa = 0.9$, $Q = 1$, $\omega_f = 1$, and $p = 1$ and 2.5.

the equilibrium point (0, 0). Therefore, we write the restoring force term of (8) in the form

$$\begin{aligned} F(x,\dot{x}) &= \alpha(x)\,x + \beta(x)\,x^3 + \gamma(x)\,x^5 + f_1\left(\nu\dot{x}, \kappa\dot{x}^p\right) \\ &\equiv \delta(x)\,x + \epsilon(x)\,x^3 + \left(\kappa\left|\nu_1\right| + \nu\right)\dot{x} + c(x), \end{aligned} \tag{10}$$

where ν_1, $c(x)$, $\delta(x)$, and $\epsilon(x)$ can be found from

$$\begin{aligned} F_1(\delta,\epsilon,c,\nu_1) = \int_0^{\sigma} \Big(& f_1\left(\nu\dot{x}, \kappa\dot{x}^p\right) + \alpha x + \beta x^3 \\ & + \gamma x^5 + Q_0\cos\left(\omega_f t\right) \\ & - \left(\kappa\left|\nu_1\right| + \nu\right)\dot{x} - \delta x - \epsilon x^3 \\ & - c - Q_0\cos\left(\omega_f t\right)\Big)^2 dx \longrightarrow \min, \end{aligned} \tag{11}$$

$$\begin{aligned} F_2(\delta,\epsilon,c,\nu_1) = \int_0^{\upsilon} \Big(& f_1\left(\nu\dot{x}, \kappa\dot{x}^p\right) + \alpha x \\ & + \beta x^3 + \gamma x^5 + Q_0\cos\left(\omega_f t\right) \\ & - \left(\kappa\left|\nu_1\right| + \nu\right)\dot{x} - \delta x - \epsilon x^3 \\ & - c - Q_0\cos\left(\omega_f t\right)\Big)^2 d\dot{x} \longrightarrow \min, \end{aligned} \tag{12}$$

$$\partial F_1 \frac{(\delta,\epsilon,c,\nu_1)}{\partial\delta} = 0, \qquad \partial F_1 \frac{(\delta,\epsilon,c,\nu_1)}{\partial\epsilon} = 0, \tag{13}$$

$$\partial F_1 \frac{(\delta,\epsilon,c,\nu_1)}{\partial c} = 0, \qquad \partial F_2 \frac{(\delta,\epsilon,c,\nu_1)}{\partial\nu_1} = 0. \tag{14}$$

In (11) and (12), σ and υ are fitting parameters whose values must be fixed to ensure that the equivalent restoring forces are qualitatively and quantitatively similar to those of the original equations of motion. During the transformation process, the values of Q_0 and ω_f are assumed to remain constant. Once the expressions to determine ν_1, $c(x)$, $\delta(x)$, and $\epsilon(x)$ are found, then (1) can be written as the following Duffing-type equation of motion:

$$\begin{aligned} \frac{d^2x}{dt^2} + \left(\kappa\left|\nu_1\right| + \nu\right)\dot{x} + \delta(x)\,x \\ + \epsilon(x)\,x^3 + c(x) \approx Q_0\cos\left(\omega_f t\right). \end{aligned} \tag{15}$$

Notice that (1) only contains linear damping terms since the nonlinear damped effects are now contained in the $(\kappa|\nu_1| + \nu)\dot{x}$ term [18].

To assess the accuracy of the proposed solution procedure, we will next examine the dynamics response of forced oscillators with nonlinear damping terms such as the Duffing equation, the cubic-quintic Duffing equation, the rational form elastic term oscillator, and the finite extensibility nonlinear oscillator (FENO).

3. Forced Duffing Equation with Nonlinear Damping

Here we consider the forced, damped Duffing equation given by (9) and introduce the following change of variable $x = A/y$ which transforms it into an equation of the form

$$\begin{aligned} \ddot{x} + \nu\dot{x} + \kappa\dot{x}|\dot{x}|^{p-1} + Ax + Bx^3 = Q\cos\left(\omega_f t\right), \\ \text{with } x(0) = 1,\ \dot{x}(0) = 0, \end{aligned} \tag{16}$$

where $\kappa = \kappa_0 x_0^{(p-1)}$ and $Q = Q_0/x_0$. We next use (12) and (14) to derive the following forced, damped Duffing equation of the form

$$\ddot{x} + \left(\kappa\left|\nu_1\right| + \nu\right)\dot{x} + Ax + Bx^3 + c = Q\cos\left(\omega_f t\right), \tag{17}$$

where c and ν_1 are given by

$$\begin{aligned} c &= -\frac{2\kappa(p-1)\,\upsilon^p}{p+2}, \\ \nu_1 &= \frac{3p\upsilon^{(p-1)}}{\sqrt{4+4p+p^2}}. \end{aligned} \tag{18}$$

Here the values of υ must satisfy (12). To assess the accuracy of (17) when compared to the numerical integration of (16), let us consider the parameter values of $A = 1$, $B = 1$, $\nu = 0.1$, $\kappa = 0.9$, $Q = 1$, and $\omega_f = 1$ with $p = 0.1$, 0.387, 1.5, and 2.5 with the initial conditions of $x(0) = 1$ and $\dot{x}(0) = 0$. Figure 2 shows the comparison of the amplitude-time curves obtained from the numerical integration solutions of (16) and (17). As we can see from these amplitude-time plots, the predicted curves obtained from (17) follow well the numerical integration solutions of (16). In fact, the computed root-mean-square error (RMSE) values are 0.1196, 0.0874, 0.1530, and 0.1351 for the p values of 0.1, 0.387, 1.5, and 2.5, respectively. In Figure 2, the solid lines represent the numerical integration solutions of (16), while the dashed lines represent the numerical integration solutions of (17). Therefore, we can conclude that our solution procedure provides an equivalent

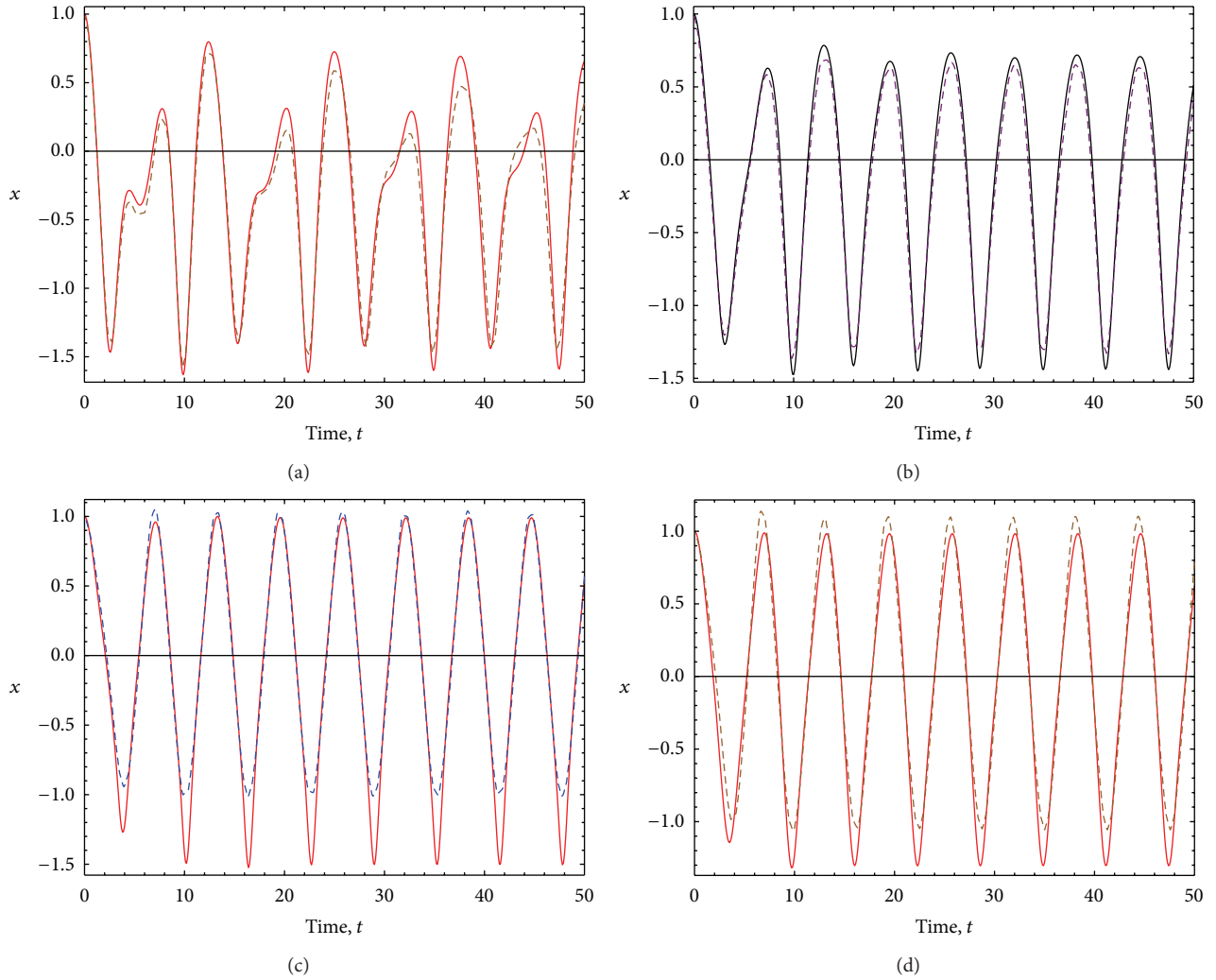

FIGURE 2: Amplitude-time response curves of (16) and (17). Here, the solid lines represent the numerical integration solutions of (16), while the dashed lines represent the numerical integration solutions of (17). The parameter values are $A = 1$, $B = 1$, $\nu = 0.1$, $\kappa = 0.9$, $Q = 1$, and $\omega_f = 1$, with $x(0) = 1$ and $\dot{x}(0) = 0$. (a) $p = 0.1$, $c = 0.8535$, $\nu_1 = 0.0574$, and $\upsilon = 2.75$; (b) $p = 0.387$, $c = 0.5544$, $\nu_1 = 0.3646$, and $\upsilon = 1.6$; (c) $p = 1.5$, $c = -0.0221$, $\nu_1 = 0.5677$, and $\upsilon = 0.195$; (d) $p = 2.5$, $c = -0.0434$, $\nu_1 = 0.3451$, and $\upsilon = 0.35$.

equation of motion that describes the dynamics behavior of the oscillatory system (16) well even when nonlinear damping terms are considered.

To further assess the accuracy of our proposed approach, we will next study the forced cubic-quintic Duffing oscillator with linear and nonlinear damping terms.

4. Cubic-Quintic Duffing Equation with Nonlinear Damping Terms

In this case, we derive the equivalent representation form of the cubic-quintic oscillator in which nonlinear damping terms are considered. Here, we assume that the equation of motion has the form

$$\ddot{y} + 2\nu\dot{y} + \eta_0 y^2 \dot{y} + \kappa_0 \dot{y}|\dot{y}|^{p-1} + \alpha y + \beta y^3 + \gamma y^5 = Q_0 \cos\left(\omega_f t\right), \tag{19}$$

with initial conditions given by $y(0) = y_0$ and $\dot{y}(0) = 0$. In (19) y denotes the displacement of the system, ν, η_0, and κ_0 are damping coefficients, α, β, and γ are system constant parameters, and Q_0 and ω_f are the driving force and frequency, respectively. Notice that the nonlinear damping terms $\eta_0 y^2 \dot{y} + \kappa_0 \dot{y}|\dot{y}|^{p-1}$ of (19) are commonly used to model the dynamics of nanoresonators and microresonators. See [3–5] and references cited therein. If we let $x = A/y$, thus, (19) becomes

$$\ddot{x} + 2\nu\dot{x} + \eta x^2 \dot{x} + \kappa\dot{x}|\dot{x}|^{p-1} + Ax + Bx^3 + Gx^5 = Q\cos\left(\omega_f t\right), \tag{20}$$

with $x(0) = 1$, $\dot{x}(0) = 0$, $A = \alpha$, $B = \beta y_0^2$, $G = \gamma y_0^4$, $\eta = \eta_0 y_0$, $\kappa = \kappa_0 y_0^{(p-1)}$, and $Q = Q_0/y_0$. In accordance with our proposed nonlinear transformation approach, the system terms

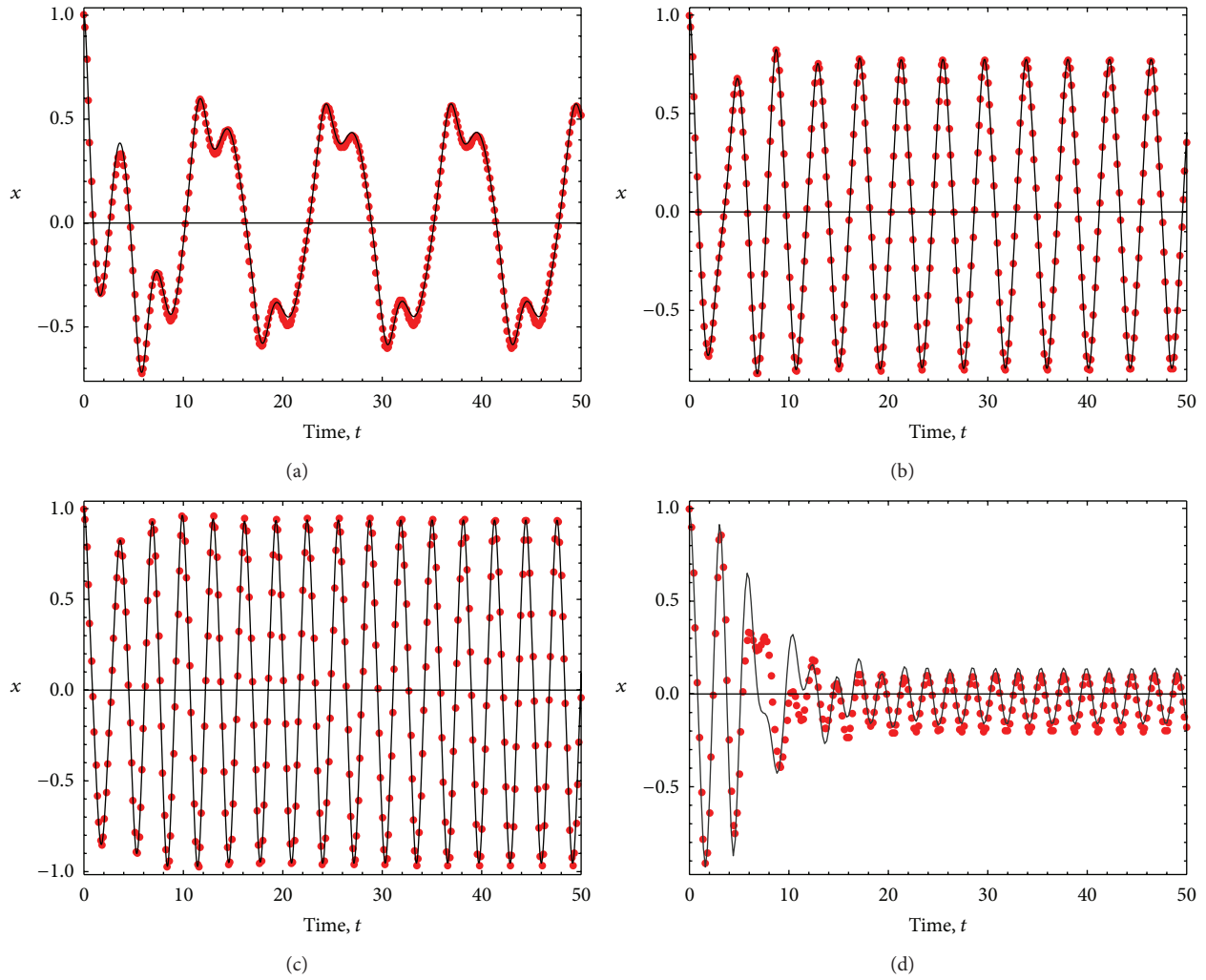

FIGURE 3: Amplitude-time response curves of (19) and (22). The parameter values are $\alpha = 1$, $\beta = 5$, $\gamma = 1$, $\nu = 0.1$, $\eta_0 = 0.15$, $\kappa_0 = 0.25$, $Q = 1$, $p = 3/4$, and $\omega_f = 0.5$, 1.5, 2, and 2.75 with $x(0) = 1$ and $\dot{x}(0) = 0$. The computed parameter values are $\delta = 0.9147$, $\epsilon = 5.5863$, $\nu_1 = 1.395$, $c = 0.0572$, $\sigma = 0.685$, and $\upsilon = 0.05$. (a) Amplitude-time response curves for $\omega_f = 0.5$; (b) amplitude-time response curves for $\omega_f = 1.5$; (c) amplitude time-response curves for $\omega_f = 2$; (d) amplitude-time response curves for $\omega_f = 2.75$. Here the solid black lines represent the numerical integration solution of (19) while the red dots represent the prediction obtained by using the derived equivalent equation of motion (22).

$2\nu\dot{x}+\eta x^2\dot{x}+\kappa\dot{x}^p+Ax+Bx^3+Gx^5$ are replaced by an equivalent cubic-like polynomial expression of the form

$$\begin{aligned} &2\nu\dot{x} + \eta x^2\dot{x} + \kappa\dot{x}|\dot{x}|^{p-1} + Ax + Bx^3 + Gx^5 \\ &\quad\equiv \left(\kappa\left|\nu_1\right| + \nu\right)\dot{x} + \delta x + \epsilon x^3 + c. \end{aligned} \tag{21}$$

Thus, the equivalent nonlinear transformation form of (20) is given as

$$\ddot{x} + \left(\kappa\left|\nu_1\right| + \nu\right)\dot{x} + \delta x + \epsilon x^3 + c \approx Q\cos\left(\omega_f t\right), \tag{22}$$

where

$$\begin{aligned} \delta &= A + \frac{5\eta\upsilon\sigma}{12} - \frac{25G\sigma^4}{63}, \\ \epsilon &= B + \frac{5\left(21\eta\upsilon + 40G\sigma^3\right)}{162\sigma}, \\ \nu_1 &= \frac{3p\upsilon^{p-1}}{2+p} + \frac{252\upsilon\nu + 273\eta\upsilon\sigma^2 - 80G\sigma^5}{252\kappa\upsilon}, \\ c &= -\frac{2\kappa\left(p-1\right)\upsilon^p}{2+p} + \frac{848G\sigma^5 - 2541\eta\upsilon\sigma^2}{2268}. \end{aligned} \tag{23}$$

To evaluate the accuracy of (22), we use the parameter values of $\alpha = 1$, $\beta = 5$, $\gamma = 1$, $\nu = 0.1$, $\eta_0 = 0.15$, $\kappa_0 = 0.25$, $Q = 1$, and $\omega_f = 0.5, 1.5, 2$, and 2.75 with the initial conditions of $x(0) = 1$ and $\dot{x}(0) = 0$. Figure 3 illustrates the amplitude versus time plots by considering a nonlinear damping term of order $p = 3/4$. The solid black lines represent the numerical integration of (19) while the red dots represent the numerical

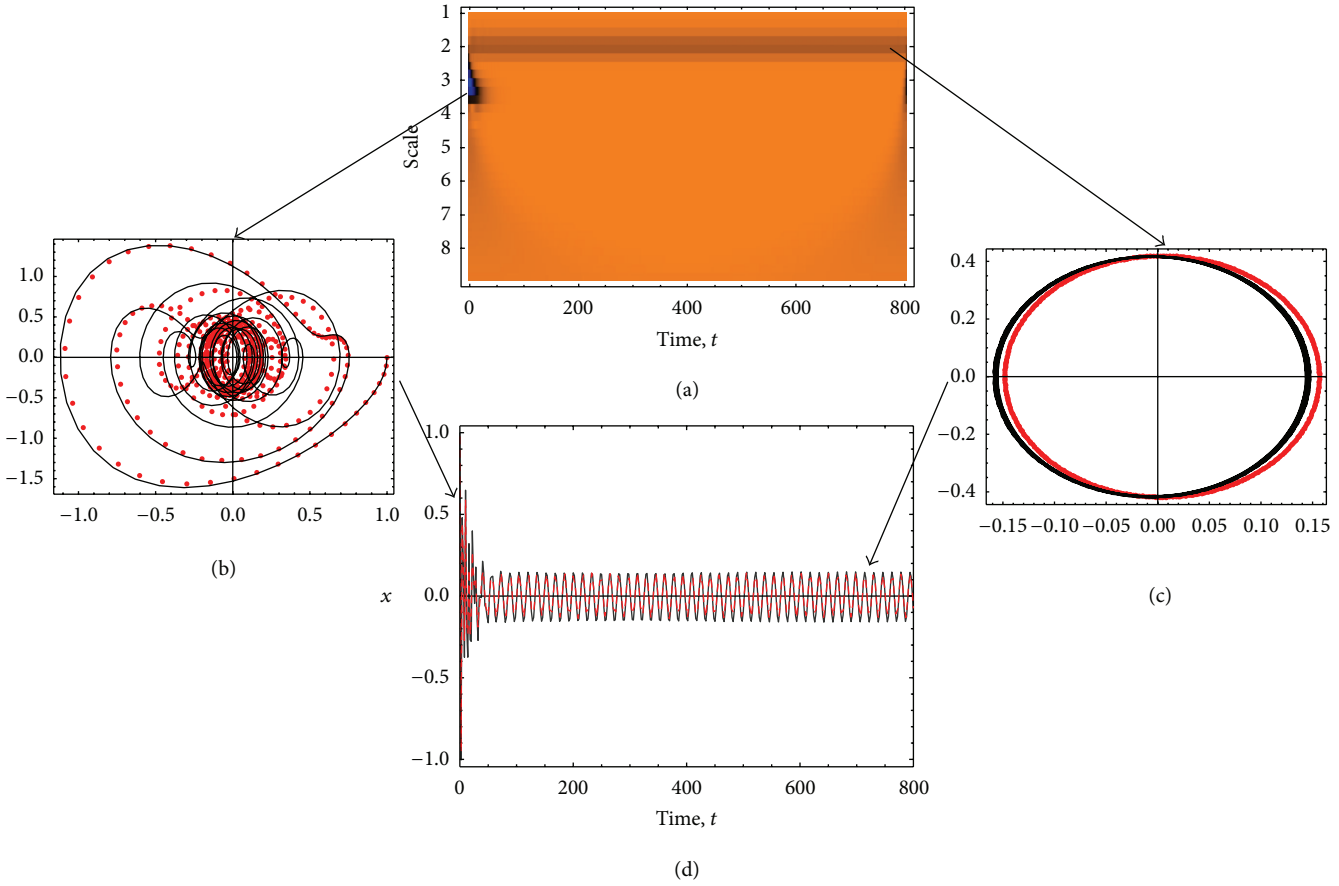

FIGURE 4: Amplitude-time response curves of (19) and (22). The parameter values are $\alpha = 1$, $\beta = 1$, $\gamma = 0.1$, $\upsilon_0 = 0.05$, $\eta_0 = 0.15$, $\kappa_0 = 0.1$, $\omega_f = 2.75$, and $Q = 1$, with $x_0 = 1$ and $\dot{x}(0) = 0$. Here $\delta = 0.9975$, $\epsilon = 1.0679$, $\upsilon_1 = 1.2806$, and $c = -0.0045$, with $\sigma = 0.645$ and $\upsilon = 0.11$. (a) Morlet continuum wavelet transform plot; (b) transient response phase portrait on $0 \leqslant t \leqslant 50$; (c) the steady-state system response phase portrait on $750 \leqslant t \leqslant 800$; (d) amplitude-time response curves. Here the solid lines represent the numerical integration solution of (19), while the red dots represent predicted values obtained by using the derived equivalent equation of motion (22).

integration of (22). Notice that in all cases, the predicted solutions obtained from (22) follow well the numerical integration solution of the original equation of motion. The computed parameter values are $\delta = 0.9147$, $\epsilon = 5.5863$, $\nu_1 = 1.395$, $c = 0.0572$, $\sigma = 0.685$, and $\upsilon = 0.05$. In all cases, the maximum RMSE value does not exceed 0.0666. As a second example, let us consider the following system parameter values: $\alpha = 1$, $\beta = 1$, $\gamma = 0.1$, $\nu_0 = 0.05$, $\eta_0 = 0.15$, $\kappa_0 = 0.1$, $\omega_f = 2.75$, and $Q = 1$. Here the computed values for δ, ϵ, ν_1, and c are, respectively, 0.9975, 1.0679, 1.2806, and −0.0045 with $\sigma = 0.645$ and $\upsilon = 0.11$. The corresponding RMSE value computed on $0 \leqslant t \leqslant 800$ is 0.0188. Figure 4 illustrates the amplitude-time response curves, the phase space, and the Morlet continuum wavelet transform plots. As usual, the solid black lines represent the numerical integration of (20) while the red dots describe the numerical integration solution of (22). From these plots, it is clear that the equivalent representation form (22) of (20) describes well the system dynamics response. Of course, the equivalent expression (22) can be used if different system parameter values are considered.

We will next derive the equivalent representation form of the forced power-form elastic term oscillator with linear and nonlinear damping terms.

5. The Forced Power-Form Elastic Term Oscillator with Nonlinear Damping

The equation of motion of this oscillator is assumed to be given as

$$\frac{d^2y}{dt^2} + 2\nu\frac{dy}{dt} + \kappa_0\dot{y}\left|\dot{y}\right|^{p-1} + \omega_n^2 y + h\,\mathrm{sgn}\left(y\right)\left|y\right|^m = Q_0\cos\left(\omega_f t\right), \quad y\left(0\right) = A,\ \dot{y}\left(0\right) = 0, \tag{24}$$

where ω_n, ν, κ_0, and h are constant parameters and m can take any nonnegative real value on $0 \leq m < \infty$ [31, 32]. By

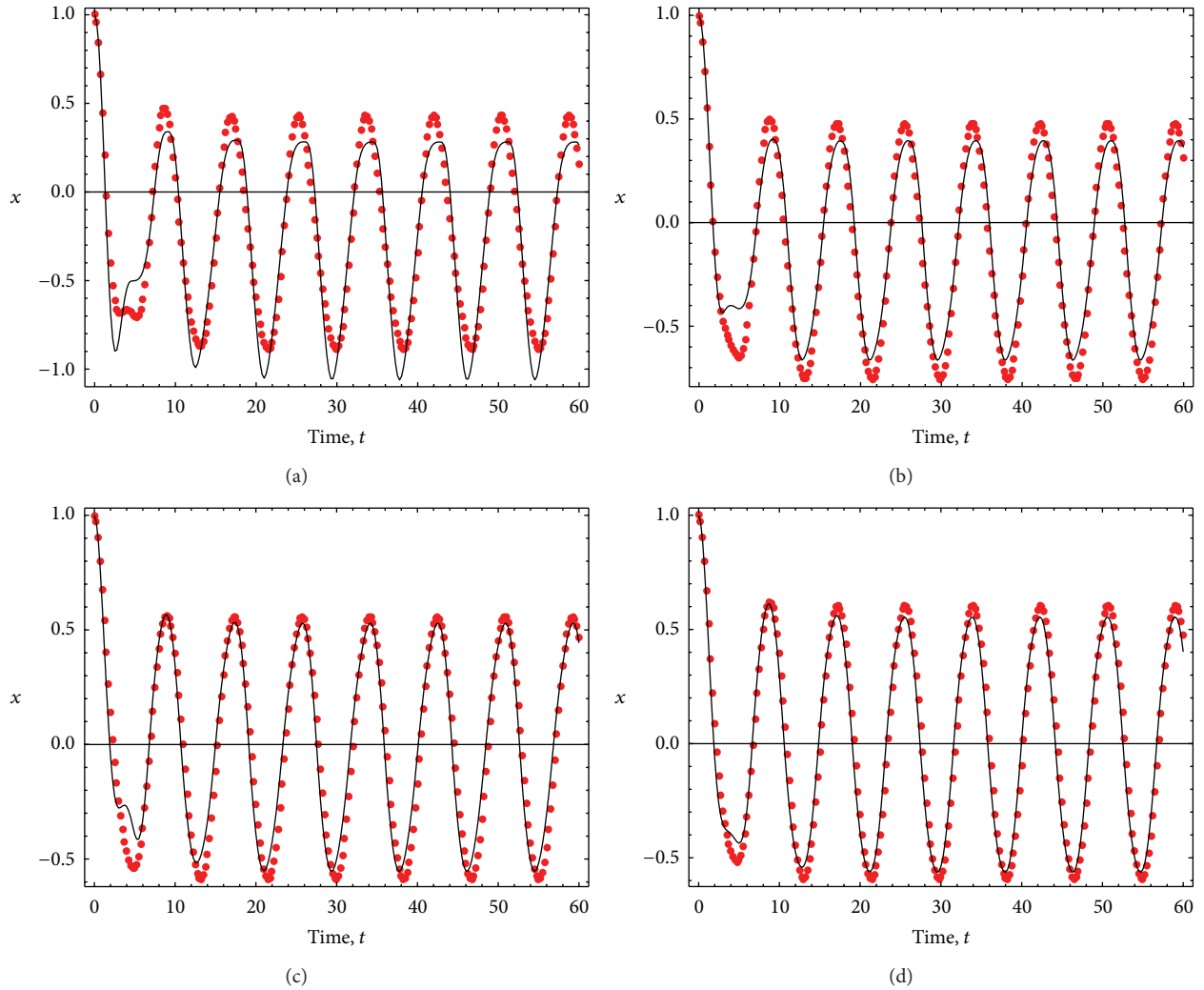

Figure 5: Amplitude-time response curves of (25) and (29). The parameter values are $m = 3/2$, $A = 1$, $\omega_n = 1$, $h = 1$, $Q_0 = 1$, $\nu = 0.1$, $\kappa = 0.9$, and $\omega_f = 0.75$, with $x_0 = 1$ and $\dot{x}(0) = 0$. (a) Amplitude-time response curves for $p = 1/4$; (b) amplitude-time response curves for $p = 3/4$; (c) amplitude time-response curves for $p = 1.5$; (d) amplitude-time response curves for $p = 2.75$. Here the solid black lines represent the numerical integration solution of (25), while the red dots represent the prediction obtained by using the derived equivalent equation of motion (29).

introducing the coordinate transformation $x = y/A$, (24) can be written as

$$\begin{aligned} &\frac{d^2x}{dt^2} + 2\nu\frac{dx}{dt} + \kappa\dot{x}|\dot{x}|^{p-1} + \omega_n^2 x \\ &\quad + c_1\,\mathrm{sgn}\,(x)\,|x|^m = Q\cos\left(\omega_f t\right), \\ &\text{with } c_1 = hA^{(m-1)},\ \kappa = \kappa_0 A^{(p-1)}, \\ &Q = \frac{Q_0}{A}\quad x\,(0) = 1,\ \dot{x}\,(0) = 0. \end{aligned} \tag{25}$$

The restoring conservative forces $\omega_n^2 x + c_1\,\mathrm{sgn}(x)|x|^m$ can be replaced by a cubic-quintic polynomial by using the Chebyshev polynomial expansion (2) which provides

$$\omega_n^2 x + c_1\,\mathrm{sgn}\,(x)\,|x|^m \approx \alpha_2 x + \beta x^3 + \gamma x^5 + \Delta x^7 + \varepsilon x^9, \tag{26}$$

where

$$\begin{aligned} \alpha_2 &= \frac{5c_1\,(m-9)\,(m-7)\,(m-5)\,(m-3)\,\Gamma\,[m/2+1]}{8\sqrt{\pi}\Gamma\,[(11+m)/2]} + \omega_n^2, \\ \beta &= -\frac{10c_1\,(m-9)\,(m-7)\,(m-5)\,(m-1)\,\Gamma\,[m/2+1]}{\sqrt{\pi}\Gamma\,[(11+m)/2]}, \\ \gamma &= \frac{42c_1\,(m-9)\,(m-7)\,(m-3)\,(m-1)\,\Gamma\,[m/2+1]}{\sqrt{\pi}\Gamma\,[(11+m)/2]}, \\ \Delta &= -\frac{64c_1\,(m-9)\,(m-5)\,(m-3)\,(m-1)\,\Gamma\,[m/2+1]}{\sqrt{\pi}\Gamma\,[(11+m)/2]}, \\ \varepsilon &= \frac{32c_1\,(m-7)\,(m-5)\,(m-3)\,(m-1)\,\Gamma\,[m/2+1]}{\sqrt{\pi}\Gamma\,[(11+m)/2]}. \end{aligned} \tag{27}$$

Table 1: Computed values of the forced power-form elastic term oscillator with nonlinear damping term. The assumed parameter values are $m = 3/2$, $A = 1$, $\omega_n = 1$, $h = 1$, $Q_0 = 1$, $\nu = 0.1$, $\kappa = 0.9$, and $\omega_f = 3/4$.

p	δ	ϵ	c	ν_1	σ	υ	RMSE
1/4	2.2003	−0.3094	0.5011	0.3964	−1	1.85	0.1293
3/4	2.2003	−0.3094	0.0609	0.8878	−1	1.85	0.0730
3/2	2.2260	−0.3513	0.0320	0.9539	0.95	0.6	0.0937
11/4	2.2260	−0.3513	−0.0111	0.6684	0.96	0.6	0.0759

Here $\Gamma[\bullet]$ represents the Euler gamma function. We next use our solution procedure previously described and determine the equivalent representation form of

$$\frac{d^2x}{dt^2} + 2\nu\frac{dx}{dt} + \kappa\dot{x}|\dot{x}|^{p-1} + \alpha_2 x + \beta x^3 + \gamma x^5 + \Delta x^7 + \varepsilon x^9 = Q\cos\left(\omega_f t\right). \tag{28}$$

This gives the following equivalent equation of motion:

$$\frac{d^2x}{dt^2} + \left(\kappa\left|\nu_1\right| + \nu\right)\frac{dx}{dt} + \delta x + \epsilon x^3 + c = Q\cos\left(\omega_f t\right), \tag{29}$$

where

$$\delta = \alpha_2 - \frac{25\gamma\sigma^4}{63} - \frac{35\Delta\sigma^6}{66} - \frac{81\varepsilon\sigma^8}{143},$$

$$\epsilon = \beta + \frac{100\gamma\sigma^2}{81} + \frac{7\left(455\Delta\sigma^4 + 432\varepsilon\sigma^6\right)}{2574},$$

$$c = -\frac{2\kappa\left(p-1\right)\upsilon^p}{p+2} + \frac{212\gamma\sigma^5}{567} + \frac{71\Delta\sigma^7}{99} + \frac{712\varepsilon\sigma^9}{715},$$

$$\nu_1 = \frac{3p\upsilon^{p-1}}{p+2} + \frac{\nu}{\kappa} - \frac{14300\gamma\sigma^5 + 28665\Delta\sigma^7 + 40824\varepsilon\sigma^9}{45045\upsilon}. \tag{30}$$

To study the influence in the system dynamics of the nonlinear damping term of (24), the parameter values of $m = 3/2$, $A = 1$, $\omega_n = 1$, $h = 1$, $Q_0 = 1$, $\nu = 0.1$, $\kappa = 0.9$, $\omega_f = 0.75$, and $p = 1/4$, 3/4, 1.5, and 2.75 are considered. Figure 5 illustrates the amplitude-time response curves obtained by numerically integrating (25) and (29). As we can see from Figure 5, the numerical integration of (29) closely follows the amplitude-time response curve obtained from (25). Here, the black solid and the red dots represent, respectively, the numerical integration solution of (25) and (29). Table 1 shows the estimated RMSE values and the computed parameter values of $\delta, \epsilon, c, \nu_1, \sigma$, and υ. Based on these results, it is concluded that our equivalent representation form (29) describes well the numerical integration solution of (25).

We will next develop the equivalent representation form of the finite extensibility nonlinear oscillator with nonlinear damping terms that models the chain dynamics of polymeric materials at high extensibility.

6. The Finite Extensibility Nonlinear Oscillator (FENO)

As a final example, we now focus our attention on determining the equivalent representation form of the FENO dynamical system:

$$\frac{d^2y}{dt^2} + 2\nu\frac{dy}{dt} + \kappa\dot{y}\left|\dot{y}\right|^{p-1} + \frac{y}{\left(1 - A^2y^2\right)} = Q\cos\left(\omega_f t\right), \quad y(0) = 1,\ \dot{y}(0) = 0, \tag{31}$$

where ν and $\kappa = \kappa_0 A^{(p-1)}$ are the damping coefficients, $Q = Q_0/A$ is the driving force, ω_f represents the driving frequency, and A is the initial oscillation amplitude on $0 < A < 1$ [33]. By using Chebyshev polynomials, the conservative force of (31) can be written in equivalent form as follows

$$\frac{y}{\left(1 - A^2y^2\right)} \equiv \alpha(A)\,y + \beta(A)\,y^3 + \gamma(A)\,y^5 + \Delta(A)\,y^7 + \varepsilon(A)\,y^9, \tag{32}$$

in which

$$\alpha(A) = \frac{1}{A^{10}\sqrt{1-A^2}}\left(A^4\left(9504 - 5600\sqrt{1-A^2}\right) + A^8\left(330 - 50\sqrt{1-A^2}\right) - 4608\left(\sqrt{1-A^2} - 1\right) + 48A^6\left(25\sqrt{1-A^2} - 66\right) + 256A^2\left(35\sqrt{1-A^2} - 44\right)\right),$$

$$\beta(A) = \frac{16}{A^{10}\sqrt{1-A^2}}\left(A^6\left(2244 - 800\sqrt{1-A^2}\right) + 128A^2\left(71 - 56\sqrt{1-A^2}\right) + 3840\left(\sqrt{1-A^2} - 1\right) + A^8\left(25\sqrt{1-A^2} - 198\right) + 8A^4\left(525\sqrt{1-A^2} - 913\right)\right),$$

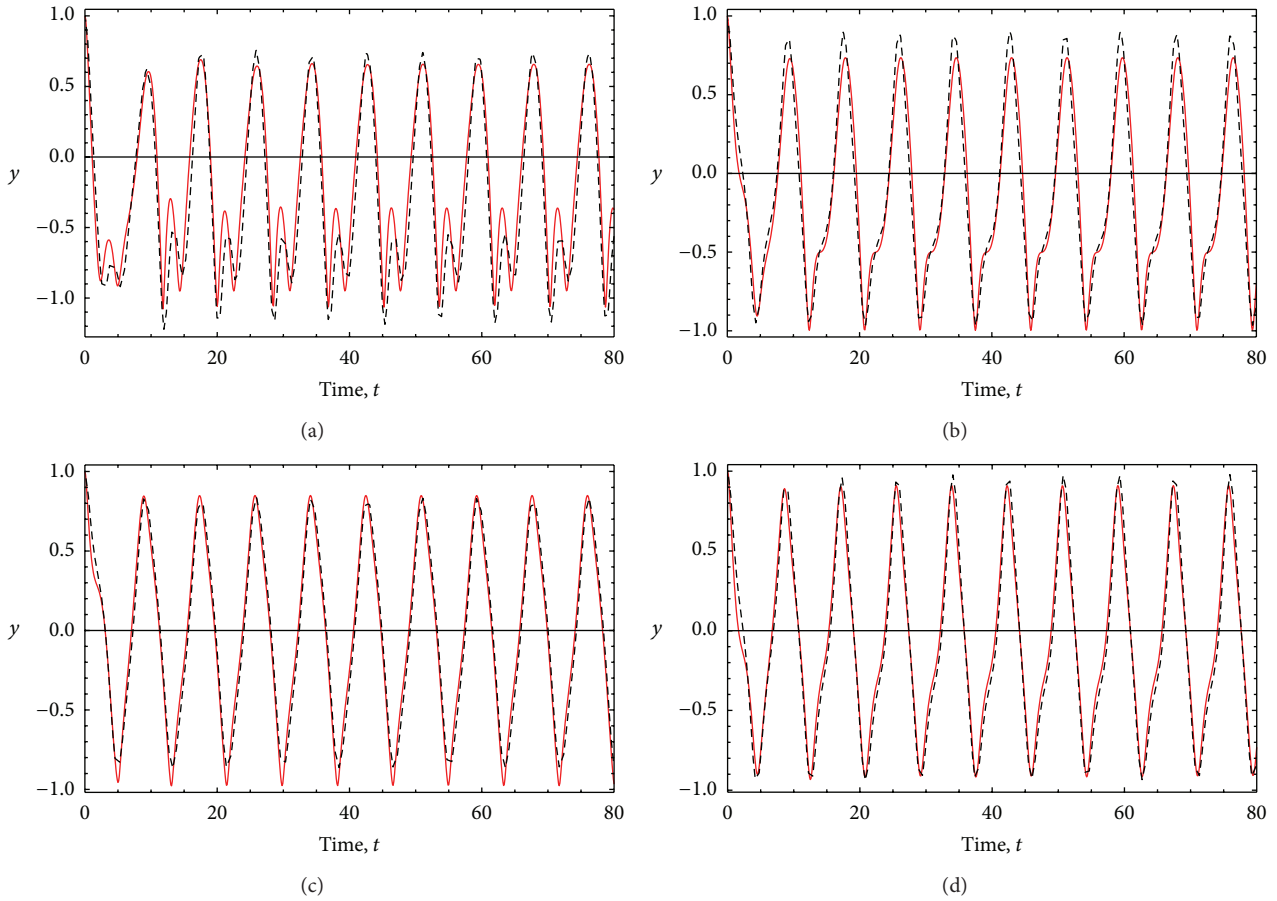

FIGURE 6: Amplitude-time response curves of (31) and (35). The parameter values are $A = 0.9$, $\nu = 0.1$, $Q_0 = 1$, and $\kappa_0 = 0.9$, with $\omega_f = 0.75$. (a) Amplitude-time response curves for $p = 1/4$; (b) amplitude-time response curves for $p = 1/2$; (c) amplitude time-response curves for $p = 1.25$; (d) amplitude-time response curves for $p = 2.5$. Here the solid black lines represent the numerical integration solution of (31) while the red dots represent the prediction obtained by using the derived equivalent equation of motion (35).

$$\begin{aligned}\gamma(A) = &-\frac{32}{A^{10}\sqrt{1-A^2}}\left(4A^6\left(913-315\sqrt{1-A^2}\right)\right.\\&+128A^2\left(125-98\sqrt{1-A^2}\right)\\&+6912\left(\sqrt{1-A^2}-1\right)\\&+A^8\left(35\sqrt{1-A^2}-297\right)\\&\left.+16A^4\left(441\sqrt{1-A^2}-779\right)\right),\end{aligned}$$

$$\begin{aligned}\Delta(A) = &\frac{256}{A^{10}\sqrt{1-A^2}}\left(64A^2\left(41-32\sqrt{1-A^2}\right)\right.\\&+8A^6\left(71-24\sqrt{1-A^2}\right)\\&+1152\left(\sqrt{1-A^2}-1\right)\\&+A^8\left(5\sqrt{1-A^2}-44\right)\\&\left.+80A^4\left(14\sqrt{1-A^2}-25\right)\right),\end{aligned}$$

$$\begin{aligned}\varepsilon(A) = &-\frac{512}{A^{10}\sqrt{1-A^2}}\left(64A^2\left(9-7\sqrt{1-A^2}\right)\right.\\&+A^8\left(\sqrt{1-A^2}-9\right)\\&-40A^6\left(\sqrt{1-A^2}-3\right)\\&+256\left(\sqrt{1-A^2}-1\right)\\&\left.+48A^4\left(5\sqrt{1-A^2}-9\right)\right).\end{aligned} \tag{33}$$

Thus, (31) becomes

$$\begin{aligned}&\frac{d^2y}{dt^2}+2\nu\frac{dy}{dt}+\kappa\dot{y}\left|\dot{y}\right|^{p-1}+\alpha(A)\,y+\beta(A)\,y^3\\&\quad+\gamma(A)\,y^5+\Delta(A)\,y^7+\varepsilon(A)\,y^9=Q\cos\left(\omega_f t\right).\end{aligned} \tag{34}$$

We next determine the Duffing-like representation form of (34) by using (11)–(14). This yields

$$\frac{d^2y}{dt^2}+\left(\kappa\left|\nu_1\right|+\nu\right)\frac{dy}{dt}+\delta y+\epsilon y^3+c=Q\cos\left(\omega_f t\right), \tag{35}$$

Table 2: Computed values of the finite extensibility nonlinear oscillator (FENO) with nonlinear damping term. The assumed parameter values are $A = 0.9$, $\nu = 0.1$, $Q_0 = 1$, and $\kappa_0 = 0.9$, with $\omega_f = 0.75$.

p	δ	ϵ	c	ν_1	σ	υ	RMSE
1/4	0.6432	2.0089	0.7490	0.2392	-0.800	4.8	0.1984
1/2	0.4782	2.3696	0.1949	0.5017	-0.875	4.8	0.1270
5/4	0.6919	1.8831	0.0371	1.0742	0.750	0.8	0.0819
3/2	0.6601	1.9668	0.0894	0.3851	0.785	0.5	0.0927

where

$$\delta = \alpha - \frac{25\gamma\sigma^4}{63} - \frac{35\Delta\sigma^6}{66} - \frac{81\varepsilon\sigma^8}{143},$$

$$\epsilon = \beta + \frac{100\gamma\sigma^2}{81} + \frac{7\left(455\Delta\sigma^4 + 432\varepsilon\sigma^6\right)}{2574},$$

$$c = -\frac{2\kappa\left(p-1\right)\upsilon^p}{p+2} + \frac{212\gamma\sigma^5}{567} + \frac{71\Delta\sigma^7}{99} + \frac{712\varepsilon\sigma^9}{715},$$

$$\nu_1 = \frac{3p\upsilon^{p-1}}{p+2} + \frac{\nu}{\kappa} - \frac{14300\gamma\sigma^5 + 28665\Delta\sigma^7 + 40824\varepsilon\sigma^9}{45045\upsilon}. \tag{36}$$

Notice that equations in (36) are similar to those derived for the forced power-form elastic term oscillator with nonlinear damping term but with different expressions to determine the values of α, β, γ, Δ, and ε.

To illustrate the accuracy attained from the derived nonlinear equivalent equation of motion of the FENO oscillator, let us consider the parameter values of ν, κ_0, Q_0, ω_f, and A to be, respectively, 0.1, 0.9, 1, 0.75, and 0.9 with $p = 0.25$, 0.5, 1.25, and 2.5. In this case $\alpha = 1.224$, $\beta = -3.1263$, $\gamma = 19.0743$, $\Delta = -31.445$, and $\varepsilon = 19.4869$. The computed values of δ, ϵ, c, ν_1, σ, and υ are summarized in Table 2. Figure 6 exhibits the amplitude-time plots computed from the numerical integration solutions of (31) and (35). Figure 6 shows that the amplitude-time response curves obtained form (35) describes well the qualitative and quantitative behavior of (31). In fact, the RMSE does not exceed the value of 0.1984. Here the black solid lines represent the numerical integration solution of (31), while the red dots represent the numerical integration results obtained from (35).

7. Conclusions

In this paper, we have introduced a nonlinear procedure to obtain the equivalent representation form of forced nonlinear oscillators that involve nonlinear damping that depends on velocity terms to the power p in which p is a positive number that can be even odd or fractional; that is, $p > 0$. Then, we have obtained the equivalent equation of motion of oscillators that are commonly used to study, among others, nanoresonators, microresonators, vibration isolators, the dynamics of the human movement, the retrofitting of existing girder bridges and arch bridge structures, and the finite extensibility nonlinear oscillator that is used to characterize chain dynamics of polymeric-like materials. The comparison among the numerical integration solutions of the original equations of motion and the equivalent ones exhibits good agreement in all the cases considered here even at larger nonlinear stiffness and damping parameter values. In fact, the computed RMSE values do not exceed of 0.1984 for all the oscillators studied here. Therefore, we can conclude that our nonlinear solution procedure which is developed to determine the equivalent representation form of forced oscillators with nonlinear stiffness and damping effects describes well the qualitative and quantitative dynamics behavior of the original equations of motion. Furthermore, the equivalent equations of the original equations of motion derived by using our nonlinear transformation approach can be used to study the system bifurcations and basins of attraction, since it provides equivalent representation forms that are close to those provided by Melnikov analysis [18].

Conflict of Interests

The authors declare that they have no conflict of interests with any mentioned identities in their paper.

Acknowledgments

This work was funded by Tecnológico de Monterrey-Campus Monterrey, through the Research Chair in Nanomaterials for Medical Devices and Research Chair in Intelligent Machines. Additional support was provided by the European Union Seventh Framework Programme (FP7 PEOPLE-2009) under the grant agreement IRSES no. 247476 and from Consejo Nacional de Ciencia y Tecnología (Conacyt), México.

References

[1] A. K. Mallik, V. Kher, M. Puri, and H. Hatwal, "On the modelling of non-linear elastomeric vibration isolators," *Journal of Sound and Vibration*, vol. 219, no. 2, pp. 239–253, 1999.

[2] C. Ho, Z. Lang, and S. A. Billings, "The benefits of nonlinear cubic viscous damping on the force transmissibility of a Duffing-type vibration isolator," in *Proceedings of the UKACC International Conference on Control 2012*, Cardiff, UK, September 2012.

[3] R. Lifshitz and M. C. Cross, *Reviews of Nonlinear Dynamics and Complexity*, vol. 1, Wiley-VCH, New York, NY, USA, 2008, http://www.tau.ac.il/~ronlif/pubs/RNDC1-1-2008-preprint.pdf.

[4] A. Eichler, J. Moser, J. Chaste, M. Zdrojek, I. Wilson-Rae, and A. Bachtold, "Nonlinear damping in mechanical resonators made from carbon nanotubes and graphene," *Nature Nanotechnology*, vol. 6, no. 6, pp. 339–342, 2011.

[5] S. Zaitsev, O. Shtempluck, E. Buks, and O. Gottlieb, "Nonlinear damping in a micromechanical oscillator," *Nonlinear Dynamics*, vol. 67, no. 1, pp. 859–883, 2012.

[6] D. Lee and P. Taylor, *Viscous Damper Development and Future Trends*, John Wiley & Sons, New York, NY, USA, 2001.

[7] M. Martinez-Rodrigo and M. L. Romero, "An optimum retrofit strategy for moment resisting frames with nonlinear viscous dampers for seismic applications," *Engineering Structures*, vol. 25, no. 7, pp. 913–925, 2003.

[8] E. C. Kandemir and T. Mazda, "Simplified approach to nonlinear viscous damper capacity," in *Proceedings of the 8th Annual International Conference of the International Institute for Infrastructure, Renewal and Reconstruction (IIIRR '12)*, Kumamoto, Japan, August 2012.

[9] A. Karniel and G. F. Inbar, "The use of a nonlinear muscle model in explaining the relationship between duration, amplitude, and peak velocity of human rapid movements," *Journal of Motor Behavior*, vol. 31, no. 3, pp. 203–206, 1999.

[10] B. A. Kay, J. A. S. Kelso, E. L. Saltzman, and G. Schöner, "Space-time behavior of single and bimanual rhythmical movements: data and limit cycle model," *Journal of Experimental Psychology: Human Perception and Performance*, vol. 13, no. 2, pp. 178–192, 1987.

[11] L. Seren, I. Ferrer, F. Soy et al., "Designing and prototyping of new device for scapholunate ligament repair," *Procedia CIRP*, vol. 5, pp. 270–275, 2013.

[12] D. Mottet and R. J. Bootsma, "The dynamics of goal-directed rhythmical aiming," *Biological Cybernetics*, vol. 80, no. 4, pp. 235–245, 1999.

[13] G. Litak, M. Borowiec, and A. Syta, "Vibration of generalized double well oscillators," *Zeitschrift für Angewandte Mathematik und Mechanik*, vol. 87, no. 8-9, pp. 590–602, 2007.

[14] M. Borowiec, G. Litak, and A. Syta, "Vibration of the Duffing oscillator: effect of fractional damping," *Shock and Vibration*, vol. 14, no. 1, pp. 29–36, 2007.

[15] D. Delignières, D. Nourrit, T. Deschamps, B. Lauriot, and N. Caillou, "Effects of practice and task constraints on stiffness and friction functions in biological movements," *Human Movement Science*, vol. 18, no. 6, pp. 769–793, 1999.

[16] S. Lenci, G. Menditto, and A. M. Tarantino, "Homoclinic and heteroclinic bifurcations in the non-linear dynamics of a beam resting on an elastic substrate," *International Journal of Non-Linear Mechanics*, vol. 34, no. 4, pp. 615–632, 1999.

[17] M. Taylan, "The effect of nonlinear damping and restoring in ship rolling," *Ocean Engineering*, vol. 27, no. 9, pp. 921–932, 2000.

[18] J. L. Trueba, J. Rams, and M. A. F. Sanjuán, "Analytical estimates of the effect of nonlinear damping in some nonlinear oscillators," *International Journal of Bifurcation and Chaos in Applied Sciences and Engineering*, vol. 10, no. 9, pp. 2257–2267, 2000.

[19] R. S. Barbosa and J. A. T. Machado, "Describing function analysis of systems with impacts and backlash," *Nonlinear Dynamics*, vol. 29, no. 1–4, pp. 235–250, 2002.

[20] J. Y. Gu, "Nonlinear rolling motion of ship in random beam seas," *Journal of Marine Science and Technology*, vol. 12, no. 4, pp. 273–279, 2004.

[21] S. Zaitsev, R. Almog, O. Shtempluck, and E. Buks, "Nonlinear damping in nanomechanical beam oscillator," http://arxiv.org/abs/cond-mat/0503130.

[22] M. S. Siewe and U. H. Hegazy, "Homoclinic bifurcation and chaos control in MEMS resonators," *Applied Mathematical Modelling*, vol. 35, no. 12, pp. 5533–5552, 2011.

[23] H. M. Sedighi, K. H. Shirazi, and J. Zare, "An analytic solution of transversal oscillation of quintic non-linear beam with homotopy analysis method," *International Journal of Non-Linear Mechanics*, vol. 47, no. 7, pp. 777–784, 2012.

[24] A. Elías-Zúñiga and O. Martínez-Romero, "Investigation of the equivalent representation form of damped strongly nonlinear oscillators by a nonlinear transformation approach," *Journal of Applied Mathematics*, vol. 2013, Article ID 245092, 7 pages, 2013.

[25] A. Elías-Zúñiga, O. Martínez-Romero, and R. K. Córdoba-Díaz, "Approximate solution for the Duffing-harmonic oscillator by the enhanced cubication method," *Mathematical Problems in Engineering*, vol. 2012, Article ID 618750, 12 pages, 2012.

[26] A. Elías-Zúñiga and O. Martínez-Romero, "Accurate solutions of conservative nonlinear oscillators by the enhanced cubication method," *Mathematical Problems in Engineering*, vol. 2013, Article ID 842423, 9 pages, 2013.

[27] A. Beléndez, M. L. Lvarez, E. Fernndez, and I. Pascual, "Cubication of conservative nonlinear oscillators," *European Journal of Physics*, vol. 30, no. 5, pp. 973–981, 2009.

[28] A. Beléndez, D. I. Méndez, E. Fernández, S. Marini, and I. Pascual, "An explicit approximate solution to the Duffing-harmonic oscillator by a cubication method," *Physics Letters A*, vol. 373, no. 32, pp. 2805–2809, 2009.

[29] A. Beléndez, G. Bernabeu, J. Francés, D. I. Méndez, and S. Marini, "An accurate closed-form approximate solution for the quintic Duffing oscillator equation," *Mathematical and Computer Modelling*, vol. 52, no. 3-4, pp. 637–641, 2010.

[30] A. G. Ershov and T. P. Kashevarova, "Interval mathematical library based on Chebyshev and Taylor series expansion," *Reliable Computing*, vol. 11, no. 5, pp. 359–367, 2005.

[31] V. N. Pilipchuk, "Analytical study of vibrating systems with strong non-linearities by employing saw-tooth time transformations," *Journal of Sound and Vibration*, vol. 192, no. 1, pp. 43–64, 1996.

[32] V. N. Pilipchuk, "Oscillators with a generalized power-form elastic term," *Journal of Sound and Vibration*, vol. 270, no. 1-2, pp. 470–472, 2004.

[33] M. Febbo, "A finite extensibility nonlinear oscillator," *Applied Mathematics and Computation*, vol. 217, no. 14, pp. 6464–6475, 2011.